Facile room-temperature synthesis of cobalt sulphide for efficient oxygen evolution reaction

Siyu Zhao[1], Manni Yang[1], Yeshu Tan[1], Dan J.L. Brett[2], Guanjie He[1,2,3*] and Ivan P. Parkin[1*]

[1]*Christopher Ingold Laboratory, Department of Chemistry, University College London, 20 Gordon Street, London WC1H 0AJ, U.K. Email: g.he@ucl.ac.uk; i.p.parkin@ucl.ac.uk*

[2]*Electrochemical Innovation Lab, Department Chemical Engineering, University College London, London WC1E 7JE, U.K.*

[3]*School of Chemistry, University of Lincoln, Joseph Banks Laboratories, Green Lane, Lincoln, LN6 7DL, United Kingdom*

Keywords: electrocatalysts, oxygen evolution reaction, metal sulphides

Abstract

The electrolysis of water is one of the most promising strategies to produce renewable fuels and it is important to develop an energy-conserving, low-cost and easily-prepared electrocatalyst for oxygen evolution reaction (OER). In this work, Ni foam supported Co_4S_3 (Co_4S_3/NF) was fabricated by a facile one-step approach at room temperature and exhibited excellent OER performance in alkaline media. Specifically, the Co_4S_3/NF electrocatalysts showed a small overpotential of only 340 mV to reach a current density of 100 mA cm^{-2} and a Tafel slope of 71.6 mV dec^{-1} in alkaline media. More importantly, excellent stability was achieved under a constant current density of 100 mA cm^{-2} for

100 hours and the OER performance of the catalyst was improved after 1400 cycles of linear sweep voltammetry tests in alkaline media. Furthermore, the underpinning mechanism of action was studied by measuring the change of valence states for different elements to elucidate the structural evolution and active species during the electrocatalytic process.

Introduction

Water electrolysis is a promising strategy to generate high-purity hydrogen in large-scale industrial production, which is important for the green energy scenario and the safety of future energy [1-3]. Electrolysis of water consists of two half reactions, cathodic hydrogen evolution reaction (HER) and anodic oxygen evolution reaction (OER) [4]. In recent years, electrocatalysts for HER and OER have been intensively investigated and optimized in various electrolytes (acid, neutral and base) by different strategies, such as defect engineering, doping and confinement engineering [5-13]. Compared with HER with a two-electron transfer process, the pathway for the four-electron process, OER, is more sluggish with the breaking of O-H bonds and the formation of O-O bonds, which hinders the overall efficiency of the electrolysis of water [14-16]. Noble metal oxides, such as RuO_2, IrO_2, show excellent catalytic performance and are regarded as the benchmark for OER electrocatalysts [17,18]. However, the high cost, scarcity and unstable features limit the application of noble metal-based catalysts in practical use. Thus, it is important to develop low-cost, high performance and stable electrocatalysts for OER.

Compared with noble metal-based OER electrocatalysts, transition metal-based materials have been explored largely due to their high activity and abundance in Earth's crust [19]. Much effort has been devoted to developing transition metals derivatives, such as Co [20], Ni [21], Mo [22], and Fe [23] oxides [24], hydroxides [25], nitrides [26], sulphides [27] and phosphides [28] for high-performance OER electrocatalysts. Currently, some transition metal-based electrocatalysts could even outperform the benchmark precious metal OER catalysts in regard to overpotential and stability [29,30].

Transition metal sulphides (TMSs) were demonstrated as some of the most effective OER catalysts due to their unique physical and chemical properties. In addition, TMSs behave as small band gap semi-conductors and lead to good electrical conductivity [19,31]. For example, Qu *et al*. [32] developed a spinel $MnCo_2S_4$ nanowire array on Ti mesh by the sulfidation of $MnCo_2O_4$ precursor. The catalysts showed an excellent OER activity with a small overpotential of 325 mV at a current density of 50 mA cm^{-2} in 1 M KOH, similar to that of commercial RuO_2. The Tafel slope of the material is 115 mV dec^{-1}, which implies fast OER kinetics. The catalysts also showed great stability at fixed current densities of 20 mA cm^{-2} and 50 mA cm^{-2} for 100 h. Lee *et al*. [33] developed a series of compositional tunable $Co_xNi_yS_z$ by the template-assisted method. CoO@Co_9S_8 core-shell structure was achieved by the sulphidation of CoO and the addition of Ni precursor could promote the transition from Co_9S_8 to Ni_9S_8. Then the $Co_xNi_yS_z$ could be achieved by controlling the amount of Ni precursors and the reaction time. The optimized $Co_{9-x}Ni_xS_8$ catalysts showed an overpotential of 362 mV at a current density of 10 mA cm^{-2} in 1 M NaOH and the corresponding Tafel slope

is 74.7 mV dec^{-1}. However, the instability and surface reconstruction behaviour of metal sulphides during OER requires further study to uncover the specific active species.

In this work, we report the fabrication of Ni foam supported Co_4S_3 nanostructures (Co_4S_3/NF) by a single-step wet chemistry synthesis method at room temperature, which does not require external heating or annealing processes and is a low energy-process. Meanwhile, the wet chemistry synthesis provides a promising route to synthesize transition metal sulphide materials at room temperature for large-scale production, which has great potential for industrial application. Owing to the unique electronic structures that endow rich active sites, the Co_4S_3/NF catalysts showed a small overpotential of 340 mV to reach a current density at 100 mA cm^{-2} in 1M KOH and with a small Tafel slope of 71.6 mV dec^{-1}. Furthermore, the catalysts showed excellent stability and possessed a stable output at a large current density of 100 mA cm^{-2} for 100 hours in 1M KOH. The 1400 cycles of linear sweep voltammetry tests showed an even better performance afterwards. The surface reconstruction behaviour behind the outstanding stability was investigated by *ex-situ* XPS, which showed Co^{3+}/Ni^{3+}-sulphate/sulphites species and the formed Co^{3+}/Ni^{3+}-(oxy)hydroxide contributed to the improved performance.

Experimental

Material

Cobalt chloride hexahydrate ($CoCl_2 \cdot 6H_2O$) was purchased from Sigma-Aldrich (UK) Co., Ltd. Sodium thiosulfate ($Na_2S_2O_3$) was purchased from Sigma-Aldrich (UK)

Co., Ltd. Potassium hydroxide (KOH) was purchased from Sigma-Aldrich (UK) Co., Ltd. Ni foam were used as received. All chemicals were used as received without further purification.

Preparation of $Co_4S_3/Ni(OH)_2$ supported on Ni foam ($Co_4S_3/Ni(OH)_2$@NF)

The $Co_4S_3/Ni(OH)_2$ catalysts supported on Ni foam were prepared by a one-step solution phase method at room temperature. The solution was prepared by dissolving 3g $CoCl_2 \cdot 6H_2O$ and 0.2g $Na_2S_2O_3$ into 10 ml DI water in a small bottle. Then the Ni foam (1×2 cm^2) was put into the bottle and left at room temperature for 1 day. Finally, the as-prepared samples were washed with DI water three times followed by a vacuum drying process for 12 hours. The obtained electrodes were denoted as Co_4S_3/NF. The amount of Co precursors was optimized by changing the amount of $CoCl_2 \cdot 6H_2O$ to 1g, 2g, 4g, 5g and 6g while other steps were the same and the prepared electrodes were denoted as Co_4S_3/NF-1, Co_4S_3/NF-2, Co_4S_3/NF-4, Co_4S_3/NF-5 and Co_4S_3/NF-6, respectively. The loading mass of active materials are shown in Table S1.

Characterization

Scanning electron microscope (SEM) (Joel 6700) was applied to study the morphologies of materials and Energy-Dispersive X-ray Spectroscopy (EDS) was applied to study the distribution of elements of the material. A STOE SEIFERT diffractometer with Mo X-ray source was applied to obtain the X-ray Diffraction (XRD) patterns for understanding the phase information of catalysts. X-ray Photoelectron Spectroscopy (XPS; Thermo scientific K-alpha photoelectron spectrometer) was applied to study the valence states of elements on the surface of the catalysts and the

data were analyzed by CasaXPS software.

Electrochemical tests

A three-electrode cell was used to measure the electrochemical performance of the prepared electrodes. A graphite rod and an Ag/AgCl (saturated KCl) electrode were used as the counter electrode and the reference electrode separately. The prepared self-standing electrodes were used as working electrodes directly. The Ar-saturated 1 M KOH solution was prepared and used as the electrolyte. A Gamry Interface 1000 potentiostat was used to conduct the electrochemical measurements. Linear Sweep Voltammetry (LSV) data were collected at a scan rate of 10 mV s^{-1}. The measured potentials versus Ag/AgCl electrode were converted into potentials versus reversible hydrogen electrode (RHE) by $E_{RHE} = E_{Ag/AgCl} + 0.197 + 0.059pH$. Tafel slopes were obtained by calculating the slope of corresponding replotted polarization curves. The long-term stability was evaluated by the chronovoltammetry measurement and 1400 cycles of LSV scans. Electrochemical impedance spectroscopy (EIS) was performed with frequencies from 100 kHz to 100 mHz. All the LSV measurements are presented with iR compensation.

Results and Discussion

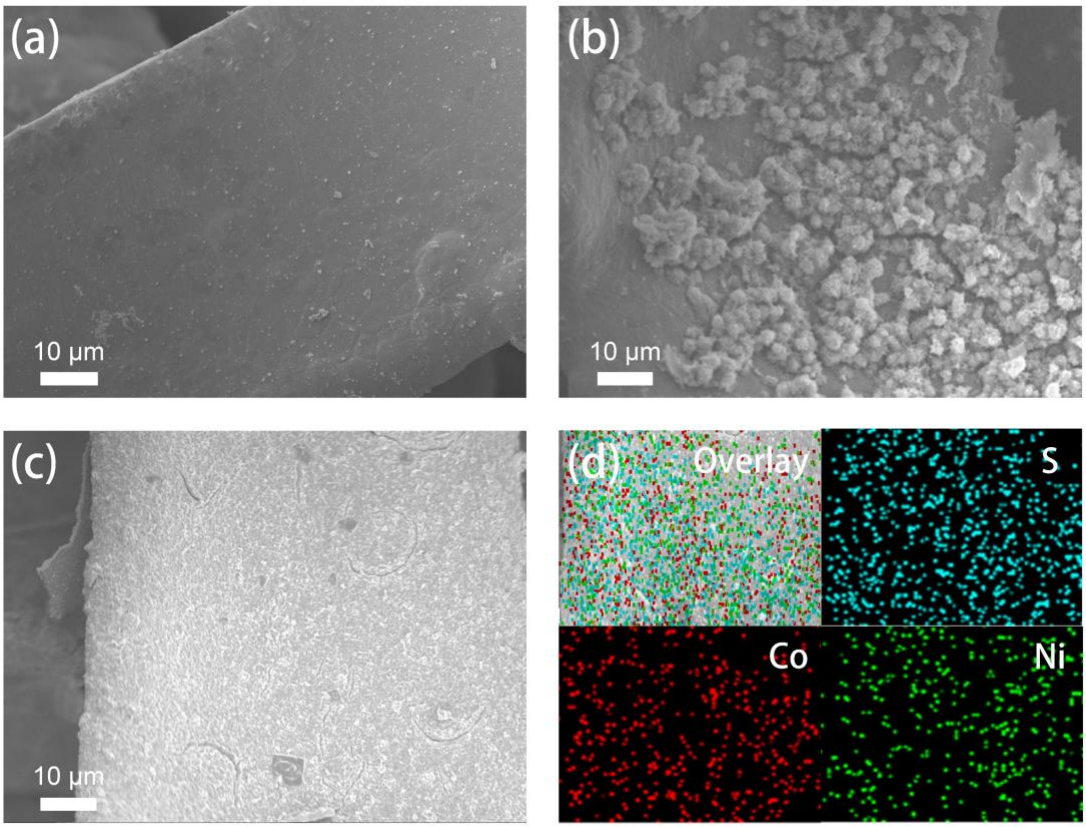

Figure 1. SEM images of (a) Co_4S_3/NF-1, (b) Co_4S_3/NF-2 and (c) Co_4S_3/NF. (d) Elemental mappings of Co_4S_3/NF.

A series of Co_4S_3/NF in this work were synthesized *via* a simple and scalable one-pot wet chemistry synthesis method. Generally, specific amounts of $CoCl_2 \cdot 6H_2O$ and $Na_2S_2O_3$ were dissolved in 10 ml of deionized water in a 15 ml glass vial. Then a piece of Ni foam was immersed in the solution and kept at room temperature for 24 hours. The colour of the electrode become darker after the reaction. Finally, the electrodes were collected and washed with DI water for several times. The as-prepared materials were used directly as self-standing OER electrodes. This method is energy-conserving, easy to operate and showed great potential for the large-scale fabrication of electrode

materials.

Cobalt precursors (1g, 2g, 3g) were applied to obtain different electrocatalysts and denoted as Co_4S_3/NF-1, Co_4S_3/NF-2 and Co_4S_3/NF, respectively. A digital photo of electrodes prepared with different amount of Co precursors is shown in Figure S1. The morphologies of electrodes and the distribution of elements were studied by Scanning Electron Microscopy (SEM) and Energy-Dispersive X-ray Spectroscopy (EDX). The material barely grows on nickel foam for Co_4S_3/NF-1, which could also be demonstrated by SEM images in Figure 1a and Figure S2. Figure 1b and Figure S3 showed the SEM images of Co_4S_3/NF-2. The colour of the electrode is darker than Co_4S_3/NF-1 and clusters of nanoparticles could be seen grown on the Ni foam skeleton. However, the materials grow unevenly on the surface of the Ni foam, which could not provide sufficient active sites for OER and thus weaken the performance. When using 3g of Co precursor, the materials grow evenly on the surface of Ni foam and the colour is the darkest which indicates uniform and dense growth of active materials on the electrode. The SEM images of Co_4S_3/NF (Figure 1c and Figure S4) provided excellent growth of the active materials on Ni foam without blocking the 3D porous structures of Ni foams, which could provide sufficient channels for the diffusion of electrolytes and promote the OER performance. The Energy-Dispersive X-ray Spectroscopy (EDX) mapping results showed a uniform distribution of the Co, S and Ni elements (Figure 1d). Therefore, the optimum amount of precursor is 3 g, was used for further analysis unless otherwise indicated.

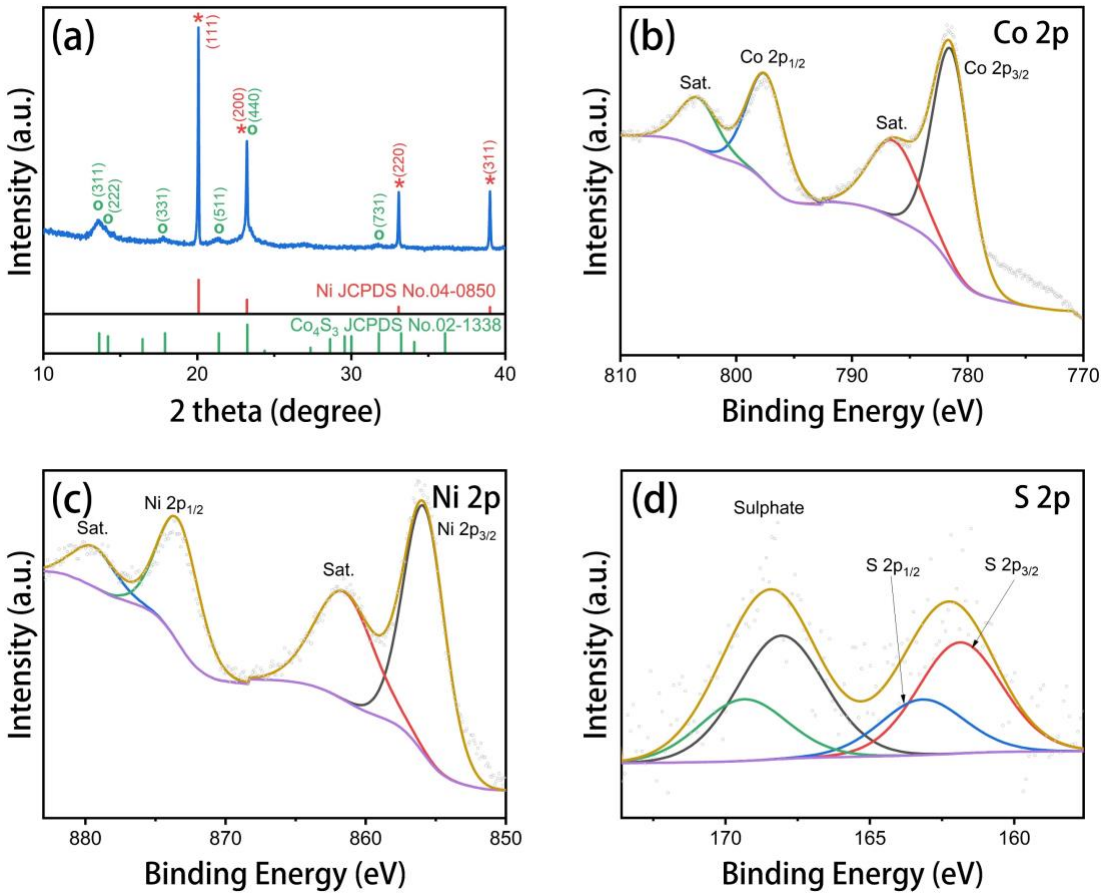

Figure 2. (a) XRD patterns of Co_4S_3/NF. XPS spectra of (b) Co 2p, (c) Ni 2p and (d) S 2p of Co_4S_3/NF.

X-ray diffraction (XRD) patterns of the Co_4S_3/NF electrodes are shown in Figure 2a. As can be seen, the XRD peaks of the electrodes at 20.1°, 23.2°, 33.1° and 39.0° could be indexed to (111), (200), (220) and (311) planes of Ni (PDF No. 04-0850). The XRD peaks at 13.6°, 17.9° and 21.4° were assigned to (311), (331) and (511) planes of Co_4S_3 (PDF No. 02-1338). The XRD results indicated the main structure of Co_4S_3/NF was Co_4S_3 with strong Ni peaks originating from the Ni foam.

The elemental valence states of the as-prepared catalysts were further investigated by X-ray photoelectron spectroscopy (XPS). The high resolution XPS spectra of Co 2p,

Ni 2p and S 2p for Co_4S_3/NF electrodes are shown in Figure 2 b-d. In the Co 2p region, two peaks at binding energies of 781.7 eV (Co $2p_{3/2}$) and 797.7 eV (Co $2p_{1/2}$) with satellite peaks of 786.8 eV and 803.5 eV were assigned to Co_4S_3 species [34]. The two peaks at binding energies of 856.0 eV (Ni $2p_{3/2}$) and 873.7 eV (Ni $2p_{1/2}$) with satellites peaks of 861.9 eV and 879.8 eV were ascribed to surface oxidized Ni^{2+} species [35]. In the S 2p region, the peak at 161.9 eV (S $2p_{3/2}$) and 163.2 eV (S $2p_{1/2}$) can be assigned to S^{2-} [36], which could be originated from Co_4S_3 species. The other two peaks at 168.1 eV (S $2p_{3/2}$) and 169.4 eV (S $2p_{1/2}$) could be assigned to a sulphate group [30], which may have come from the oxidation of residual $Na_2S_2O_3$ during the reaction or from the storage in air.

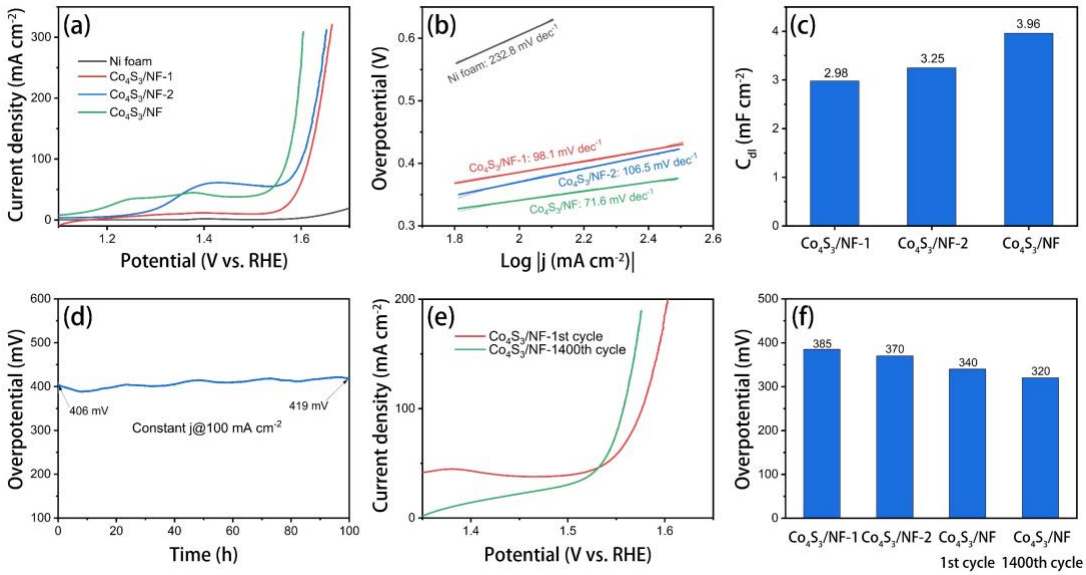

Figure 3. Electrocatalytic measurements of different electrodes for oxygen evolution in 1 M KOH. (a) The polarization curves of different samples; (b) Tafel plots derived from the curves in (a); (c) C_{dl} values of different electrodes; (d) Long-term stability test at a constant current density of 100 mA cm^{-2}; (e) Polarization curves of Co_4S_3/NF at the

1st and 1400th cycles; (f) Comparison of the overpotential to achieve 100 mA cm^{-2} for different electrodes.

The OER electrocatalytic performance of Co_4S_3/NF, Co_4S_3/NF-1, Co_4S_3/NF-2 and the pure Ni foam were examined in 1 M KOH electrolyte. Figure 3a presents the relevant polarization curves. Electrodes prepared with a larger amount of Co precursor showed better OER performance, which could be due to more active materials grown on the surface and more even distribution of the active materials. At a geometric current density of 100/300 mA cm^{-2}, the overpotential of Co_4S_3/NF is 340/373 mV, which is better than that of Co_4S_3/NF-1 (385/430 mV) and Co_4S_3/NF-2 (370/420 mV). To obtain the kinetic information of the as-prepared electrodes, the corresponding Tafel plots are provided in Figure 3b. The Co_4S_3/NF electrode exhibits a Tafel slope of 71.6 mV dec^{-1}, which is among the best reported electrodes and suggests more rapid OER catalytic kinetics (Table S2). The OER electrocatalytic performance of Co_4S_3/NF, Co_4S_3/NF-4, Co_4S_3/NF-5 and Co_4S_3/NF-6 showed a very close OER performance (Figure S5), which could be due to the saturated active materials supported on the Ni foam when preparing with more than 3g cobalt precursors. To better understand the remarkable catalytic property of Co_4S_3/NF, the electrochemically active surface area (ECSA) was investigated using a typical cyclic voltammetry (CV) method (Figure S6-S8). As shown in Figure 3c, the double-layer capacitance (C_{dl}) of Co_4S_3/NF is 3.96 mF cm^{-2}, while the C_{dl} of Co_4S_3/NF-1 and Co_4S_3/NF-2 are 2.96 mF cm^{-2} and 3.25 mF cm^{-2}, respectively. This result proved more active sites would be generated with increasing amounts of Co

precursors, corresponding to the SEM results. Figure S9 showed the EIS results of different electrodes recorded in 1 M KOH under open circuit conditions. The inherent resistance values of Co_4S_3/NF, Co_4S_3/NF-1, Co_4S_3/NF-2 and pure Ni foam are 1.304 Ω, 1.351 Ω, 1.347 Ω and 1.275 Ω, respectively. The Co_4S_3/NF electrodes showed a small value of resistance which indicated a fast electron transfer ability. On the one hand, the surface reconstruction behavior could increase the electron population on the metal center and the conductivity could be enhanced [3]. On the other hand, the large surface area and large number of pores on Ni foam could promote the mass and electron transfer [5].

Electrochemical stability is an important factor when evaluating the performance of the electrocatalysts. A chronovoltammetry test was performed on Co_4S_3/NF at a fixed current density of 100 mA cm^{-2} for 100 h. The overpotential of Co_4S_3/NF increased by 3 % from 406 mV to 419 mV after 100 h (Figure 3d), which proved the excellent stability of the catalysts. It is to be noted that the electrolyte was not replaced or refilled during the stability test. Thus, the negligible change in overpotential could be due to the decreased area of the electrodes immersed in the electrolyte, which was caused by the consumption of the electrolyte under a large current density for long working times. Furthermore, Figure 3e shows the linear sweep voltammetry test of Co_4S_3/NF for 1400 cycles in 1M KOH. Surprisingly, an enhanced OER performance was achieved after the 1400^{th} cycle. The overpotential was even lowered by 20 mV at 100 mA cm^{-2} and a lower onset potential could also be noted after stability test.

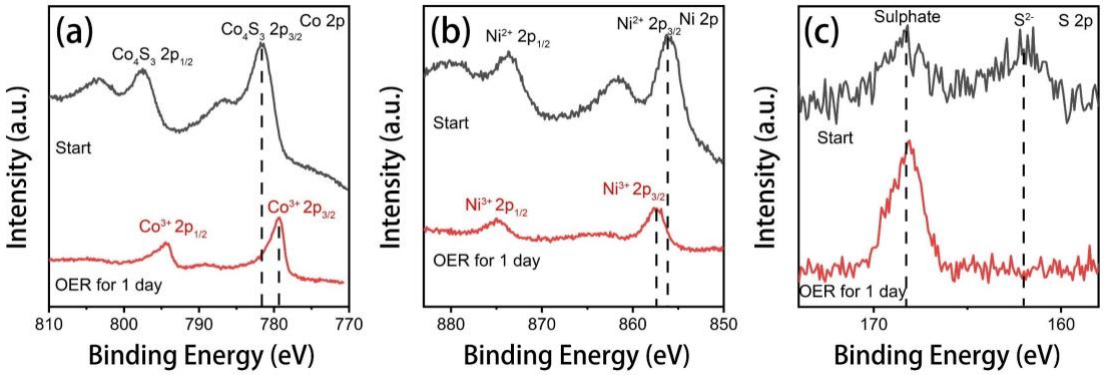

Figure 4. *Ex-situ* XPS spectra of (a) Co 2p, (b) Ni 2p and (c) S 2p of Co_4S_3/NF electrodes before and after the OER for 1 day.

To further analyze the remarkable stability of Co_4S_3/NF, an *ex-situ* XPS test was performed to study the change of valence states of the elements before and after OER tests at a constant current density of 10 mA cm^{-2} for 1 day. To avoid further possible oxidation of the materials, the electrode after the OER stability test was stored in a vacuum box before XPS analysis and transferred to XPS test chamber within 5 minutes. According to Figure 4a, by comparing the change of XPS binding energy before and after the reaction, the peaks of Co shifted to a lower binding energy, which could be due to the transformation from Co_4S_3 to Co^{3+} [37]. It is reasonable that the Co^{2+} species in Co_4S_3 are oxidized to Co^{3+} during the OER reaction. It was also observed that there was a change of binding energy of Ni before and after the reaction. The peaks of Ni shifted to a higher binding energy, which could be due to the transformation from Ni^{2+} to Ni^{3+} [38,39]. The transformation of Co and Ni could also be proved by the polarization curves of the 1st cycle of Co_4S_3/NF as shown in Figure S10. Two oxidation peaks could be seen around 1.25 V *vs*. RHE and 1.38 V *vs*. RHE, which correspond to

the oxidation peaks of Co and Ni [33]. These oxidation peaks disappeared after 1400 cycles of the LSV, which proved the total transformation of Co^{2+} and Ni^{2+} species. In the S 2p spectra, the original S^{2-} peak of the Co_4S_3 disappeared after the stability test. The changes in S XPS spectra indicates the catalyst surface undergoes a reconstruction process as the OER proceeds. The surface of the catalysts seems to change from Co_4S_3 to Co^{3+}/Ni^{3+}-sulphate/sulphites and Co^{3+}/Ni^{3+}-(oxy)hydroxide species during the OER process in the alkaline medium [30]. The XRD result of sample proved the formation of Co-sulphites species after OER stability test while the Co_4S_3 species remained, which could indicate the surface of Co_4S_3 undergoes reconstruction process (Figure S11). The morphologies of materials did not show significant changes after OER stability test (Figure S12).

Conclusions

In summary, a facile and energy-conserving method to obtain Ni foam supported Co_4S_3 at room temperature was developed. Superior electrocatalyst performance was achieved with an overpotential of 340 mV at 100 mA cm^{-2} and a Tafel slope of only 71.6 mV dec^{-1} in alkaline media. Excellent stability was realized with a negligible change in overpotential at a constant current density of 100 mA cm^{-2} for 100 hours. The LSV curves showed that the catalytic performance become even better after 1400 cycles, demonstrating excellent stability. *Ex-situ* XPS tests proved the surface reconstruction process of the catalyst and showed the Co^{3+}/Ni^{3+}-sulphate/sulphites and Co^{3+}/Ni^{3+}-(oxy)hydroxide species could be the more active species as the OER electrocatalyst.

This work provides cost-effective OER electrocatalysts with high performance and stability and provides a useful strategy to produce transition metal sulfides at room temperature.

Acknowledgement

The work was supported by Engineering and Physical Sciences Research Council (EPSRC, EP/V027433/1, EP/L015862/1, EP/R023581/1) and the Royal Society (RGS\R1\211080; IEC\NSFC\201261). S.Z. thanks the funding support from China Scholarship Council/University College London for the joint Ph.D. scholarship.

References

[1] She Z W, Kibsgaard J, Dickens C F, Chorkendorff I, Nørskov J K and Jaramillo T F 2017 Combining theory and experiment in electrocatalysis: Insights into materials design *Science*, **355**, eaad4998

[2] Zhou Z, Pei Z, Wei L, Zhao S, Jian X and Chen Y 2020 Electrocatalytic hydrogen evolution under neutral pH conditions: Current understandings, recent advances, and future prospects *Energy Environ. Sci.* **13** 3185–206

[3] Anantharaj S, Ede S R, Sakthikumar K, Karthick K, Mishra S and Kundu S 2016 Recent Trends and Perspectives in Electrochemical Water Splitting with an Emphasis on Sulfide, Selenide, and Phosphide Catalysts of Fe, Co, and Ni: A Review *ACS Catal.* **6** 8069–97

[4] Jiao Y, Zheng Y, Jaroniec M and Qiao S Z 2015 Design of electrocatalysts for oxygen- and hydrogen-involving energy conversion reactions *Chem. Soc. Rev.* **44** 2060–86

[5] Zhao S, Berry-Gair J, Li W, Guan G, Yang M, Li J, Lai F, Corà F, Holt K, Brett D J L, He G and Parkin I P 2020 The Role of Phosphate Group in Doped Cobalt Molybdate: Improved Electrocatalytic Hydrogen Evolution Performance *Adv. Sci.* **7** 1903674

[6] Zhang B, Qi Z, Wu Z, Lui Y H, Kim T H, Tang X, Zhou L, Huang W and Hu S 2019 Defect-Rich 2D Material Networks for Advanced Oxygen Evolution Catalysts *ACS Energy Lett.* **4** 328–36

[7] Tang L, Meng X, Deng D and Bao X 2019 Confinement Catalysis with 2D Materials for Energy Conversion *Adv. Mater.* **31** 1901996

[8] Lei C, Chen H, Cao J, Yang J, Qiu M, Xia Y, Yuan C, Yang B, Li Z, Zhang X, Lei L, Abbott J, Zhong Y, Xia X, Wu G, He Q and Hou Y 2018 Fe-N_4 Sites Embedded into Carbon Nanofiber Integrated with Electrochemically Exfoliated Graphene for Oxygen Evolution in Acidic Medium *Adv. Energy Mater.* **8** 1801912

[9] Zhang Y, Wu C, Jiang H, Lin Y, Liu H, He Q, Chen S, Duan T and Song L 2018 Atomic Iridium Incorporated in Cobalt Hydroxide for Efficient Oxygen Evolution Catalysis in Neutral Electrolyte *Adv. Mater.* **30** 1707522

[10] Zhu Y, Chen H C, Hsu C S, Lin T S, Chang C J, Chang S C, Tsai L D and Chen H M 2019 Operando unraveling of the structural and chemical stability of P-substituted $CoSe_2$ electrocatalysts toward hydrogen and oxygen evolution reactions in alkaline electrolyte *ACS Energy Lett.* **4** 987–94

[11] Zang Y, Niu S, Wu Y, Zheng X, Cai J, Ye J, Xie Y, Liu Y, Zhou J, Zhu J, Liu X, Wang G and Qian Y 2019 Tuning orbital orientation endows molybdenum disulfide with exceptional alkaline hydrogen evolution capability *Nat. Commun.* **10** 1217

[12] Dinh C T, Jain A, de Arquer F P G, De Luna P, Li J, Wang N, Zheng X, Cai J, Gregory B Z, Voznyy O, Zhang B, Liu M, Sinton D, Crumlin E J and Sargent E H 2019 Multi-site electrocatalysts for hydrogen evolution in neutral media by destabilization of water molecules *Nat. Energy* **4** 107–14

[13] Li G, Sun Y, Rao J, Wu J, Kumar A, Xu Q N, Fu C, Liu E, Blake G R, Werner P, Shao B, Liu K, Parkin S, Liu X, Fahlman M, Liou S C, Auffermann G, Zhang J, Felser C and Feng X 2018 Carbon-Tailored Semimetal MoP as an Efficient Hydrogen Evolution Electrocatalyst in Both Alkaline and Acid Media *Adv. Energy Mater.* **8** 1801258

[14] Chen Z, Wu R, Liu Y, Ha Y, Guo Y, Sun D, Liu M and Fang F 2018 Ultrafine Co Nanoparticles Encapsulated in Carbon-Nanotubes-Grafted Graphene Sheets as Advanced Electrocatalysts for the Hydrogen Evolution Reaction *Adv. Mater.* **30** 1802011

[15] Kang Z, Guo H, Wu J, Sun X, Zhang Z, Liao Q, Zhang S, Si H, Wu P, Wang L and Zhang Y 2019 Engineering an Earth-Abundant Element-Based Bifunctional Electrocatalyst for Highly Efficient and Durable Overall Water Splitting *Adv. Funct. Mater.* **29** 1807031

[16] Chen Z, Chen M, Yan X, Jia H, Fei B, Ha Y, Qing H, Yang H, Liu M and Wu R 2020 Vacancy Occupation-Driven Polymorphic Transformation in Cobalt Ditelluride for Boosted Oxygen Evolution Reaction *ACS Nano* **14** 6968–79

[17] Niu S, Jiang W J, Tang T, Yuan L P, Luo H and Hu J S 2019 Autogenous Growth of Hierarchical NiFe$(OH)_x$/FeS Nanosheet-On-Microsheet Arrays for Synergistically

Enhanced High-Output Water Oxidation *Adv. Funct. Mater.* **29** 1902180

[18] Tahir M, Pan L, Idrees F, Zhang X, Wang L, Zou J J and Wang Z L 2017 Electrocatalytic oxygen evolution reaction for energy conversion and storage: A comprehensive review *Nano Energy* **37** 136–57

[19] Lu F, Zhou M, Zhou Y and Zeng X 2017 First-Row Transition Metal Based Catalysts for the Oxygen Evolution Reaction under Alkaline Conditions: Basic Principles and Recent Advances *Small* **13** 1701931

[20] Moysiadou A, Lee S, Hsu C S, Chen H M and Hu X 2020 Mechanism of Oxygen Evolution Catalyzed by Cobalt Oxyhydroxide: Cobalt Superoxide Species as a Key Intermediate and Dioxygen Release as a Rate-Determining Step *J. Am. Chem. Soc.* **142** 11901–14

[21] Garcia A C, Touzalin T, Nieuwland C, Perini N and Koper M T M 2019 Enhancement of Oxygen Evolution Activity of Nickel Oxyhydroxide by Electrolyte Alkali Cations *Angew. Chemie - Int. Ed.* **58** 12999–3003

[22] Chu H, Zhang D, Jin B and Yang M 2019 Impact of morphology on the oxygen evolution reaction of 3D hollow Cobalt-Molybdenum Nitride *Appl. Catal. B Environ.* **255** 117744

[23] Bai L, Hsu C S, Alexander D T L, Chen H M and Hu X 2019 A Cobalt-Iron Double-Atom Catalyst for the Oxygen Evolution Reaction *J. Am. Chem. Soc.* **141** 14190–9

[24] Zhu Y, Tahini H A, Hu Z, Chen Z G, Zhou W, Komarek A C, Lin Q, Lin H J, Chen C Te, Zhong Y, Fernández-Díaz M T, Smith S C, Wang H, Liu M and Shao Z 2020 Boosting Oxygen Evolution Reaction by Creating Both Metal Ion and Lattice-Oxygen

Active Sites in a Complex Oxide *Adv. Mater.* **32** 1905025

[25] Cai Z, Bu X, Wang P, Ho J C, Yang J and Wang X 2019 Recent advances in layered double hydroxide electrocatalysts for the oxygen evolution reaction *J. Mater. Chem. A* **7** 5069–89

[26] Chen J, Cui P, Zhao G, Rui K, Lao M, Chen Y, Zheng X, Jiang Y, Pan H, Dou S X and Sun W 2019 Low-Coordinate Iridium Oxide Confined on Graphitic Carbon Nitride for Highly Efficient Oxygen Evolution *Angew. Chemie - Int. Ed.* **58** 12540–4

[27] Deng S, Shen Y, Xie D, Lu Y, Yu X, Yang L, Wang X, Xia X and Tu J 2019 Directional construction of Cu_2S branch arrays for advanced oxygen evolution reaction *J. Energy Chem.* **39** 61–7

[28] Zhang H, Zhou W, Dong J, Lu X F and Lou X W D 2019 Intramolecular electronic coupling in porous iron cobalt (oxy)phosphide nanoboxes enhances the electrocatalytic activity for oxygen evolution *Energy Environ. Sci.* **12** 3348–55

[29] Fei B, Chen Z, Liu J, Xu H, Yan X, Qing H, Chen M and Wu R 2020 Ultrathinning Nickel Sulfide with Modulated Electron Density for Efficient Water Splitting *Adv. Energy Mater.* **10** 2001963

[30] Yu L, Wu L, McElhenny B, Song S, Luo D, Zhang F, Yu Y, Chen S and Ren Z 2020 Ultrafast room-temperature synthesis of porous S-doped Ni/Fe (oxy)hydroxide electrodes for oxygen evolution catalysis in seawater splitting *Energy Environ. Sci.* **13** 3439–45

[31] Guo Y, Park T, Yi J W, Henzie J, Kim J, Wang Z, Jiang B, Bando Y, Sugahara Y, Tang J and Yamauchi Y 2019 Nanoarchitectonics for Transition-Metal-Sulfide-Based

Electrocatalysts for Water Splitting *Adv. Mater.* **31** 1807134

[32] Zhang X, Si C, Guo X, Kong R and Qu F 2017 A $MnCo_2S_4$ nanowire array as an earth-abundant electrocatalyst for an efficient oxygen evolution reaction under alkaline conditions *J. Mater. Chem. A* **5** 17211–5

[33] Kim J, Jin H, Oh A, Baik H, Joo S H and Lee K 2017 Synthesis of compositionally tunable, hollow mixed metal sulphide $Co_xNi_yS_z$ octahedral nanocages and their composition-dependent electrocatalytic activities for oxygen evolution reaction *Nanoscale* **9** 15397–406

[34] Ma X X and He X Q 2016 $Co_4S_3/Ni_xS_6(7 \geq x \geq 6)$/NiOOH in-situ encapsulated carbon-based hybrid as a high-efficient oxygen electrode catalyst in alkaline media *Electrochim. Acta* **213** 163–73

[35] Li S, Xi C, Jin Y Z, Wu D, Wang J Q, Liu T, Wang H Bin, Dong C K, Liu H, Kulinich S A and Du X W 2019 Ir-O-V Catalytic Group in Ir-Doped $NiV(OH)_2$ for Overall Water Splitting *ACS Energy Lett.* **4** 1823–9

[36] Wan K, Luo J, Zhou C, Zhang T, Arbiol J, Lu X, Mao B W, Zhang X and Fransaer J 2019 Hierarchical Porous Ni_3S_4 with Enriched High-Valence Ni Sites as a Robust Electrocatalyst for Efficient Oxygen Evolution Reaction *Adv. Funct. Mater.* **29** 1900315

[37] Li Z, Yuan D, Zhu S, Fan P, Ma H, Zhang Q, Wen A and Zhu J 2019 The multi-structure $NiCo_2S_4$ prepared by solvothermal method for supercapacitor accompanied with positron annihilation study *J. Appl. Phys.* **125** 175103

[38] Liu Q, Chen Q, Zhang Q, Xiao Y, Zhong X, Dong G, Delplancke-Ogletree M P, Terryn H, Baert K, Reniers F and Diao X 2018 In situ electrochromic efficiency of a

nickel oxide thin film: Origin of electrochemical process and electrochromic degradation *J. Mater. Chem. C* **6** 646–53

[39] Hao Y, Li Y, Wu J, Wang J, Jia C, Liu T, Yang X, Liu Z and Gong M 2020 Recognition of surface oxygen intermediates on NiFe oxyhydroxide oxygen-evolving catalysts by homogeneous oxidation reactivity *J. Am. Chem. Soc.* DOI: 10.1021/jacs.0c11307.